Influence of Interfacial Constraints on the Morphology of Asymmetric Crystalline-Amorphous Diblock Copolymer Films

Yuan Li,[†] Yueh-Lin Loo,[‡] Richard A. Register,[§] and Peter F. Green*[,†,‡]

Graduate Program in Materials Science and Engineering and Department of Chemical Engineering, The University of Texas at Austin, Austin, Texas 78712, and Department of Chemical Engineering, Princeton University, Princeton, New Jersey 08544

Received February 4, 2005; Revised Manuscript Received May 2, 2005

ABSTRACT: Through control of the temperature, T, and film thickness, h, the relative influence of forces associated with crystallization, long-range van der Waals forces, and block-copolymer ordering were manipulated to control the structure of films of asymmetric polyethylene-*b*-poly(styrene-*r*-ethylene-*r*-butene) (E-*b*-SEB) diblock copolymers. The bulk equilibrium structure of this copolymer consists of spheres of the crystallizable E block embedded in the amorphous SEB matrix. In thin films, the E component resides at the free surface and the SEB block resides in contact with the substrate. Within the temperature range $T > T_m$, where T_m is the melting temperature, yet below the order−disorder transition (ODT) temperature, T_{ODT}, all films of thickness $h > 12$ nm were ordered throughout. The thickness of the brush layer L_0, in contact with the substrate, of these films was 12 nm; this thickness is about one-half of the intersphere spacing of the bulk copolymer. Films equal to or thinner than 12 nm dewet, forming droplets on the substrate. However, at temperatures below the melting temperature but above the glass transition temperature of the amorphous block, films in the same thickness range ($h \leq 12$ nm) were structurally stable. While thicker films were stable as well, crystallization had a significant effect on the topography of these films, particularly as the film thickness increased.

Introduction

Interfacial forces influence the morphological structure of thin films, regardless of chemical structure. The topographies of thin films often are indicative of the nature of the dominant interfacial forces. For example, thin homopolymer (or simple) liquid films in the nanometer thickness range may be morphologically unstable or metastable because they are potentially subject to destabilizing long-range intermolecular forces.[1−5] The stability is determined by an effective interface potential, $\Phi(h)$, which has both long- and short-range contributions. Such films may rupture and form patterns that reflect the nature of the intermolecular forces. Metastable films are destabilized by nucleation and growth of holes, whereas unstable films form spinodal patterns. Typically, these patterns evolve into droplets on an underlying substrate over a sufficiently long time interval.

In the case of an A-*b*-B diblock copolymer, the situation is often more interesting because these molecules self-organize into various mesoscopic geometric arrangements of A-rich and B-rich phases (spheres, cylinders, and lamellae) below an order−disorder transition temperature (ODT).[6−14] The ODT of an A-*b*-B copolymer is determined by the total number of monomers that compose the chain, N, the Flory−Huggins interaction parameter, χ, and by the fraction of A monomers on the chain, f.[6−8,15] Interfaces influence the structure and the orientation of the phases in diblock copolymer thin films. Often, one block preferentially interacts with an interface (free surface or substrate), and this interaction determines the local segmental concentration profile.[1,16] For lamellar structures, a modulation of the concentration profile propagates normal to boundaries because the dissimilar blocks are connected. The effective interface potential of the copolymer is a periodic function of film thickness, where locations of the minima in the potential, separated by distance L, denote the stable film thicknesses.[16] For the case where a different block resides at the substrate and at the free surface (asymmetric wetting), the minima reside at locations $(n + 1/2)L$; hence, films of thickness $h = (n + 1/2)L$ remain stable, with uniform thicknesses. In the symmetric wetting case, films of $h = nL$ remain stable. When the film thickness deviates by an amount, δh, from the appropriate quantization criterion, the excess material forms a discontinuous layer of thickness L, provided the film is below the ODT. If δh is small, then the discontinuous layer forms islands, whereas as δh approaches L, the layer contains holes. In cases where the attraction of one component to the substrate occurs but the film is above the bulk ODT, then the effective interface potential is a damped oscillatory function of h and the undulations of the topographies, away from the minima, bear no relation to L.[1]

In a third situation, the molecules may exhibit a tendency to crystallize. If the molecules are homopolymers and they exhibit a tendency to crystallize, then crystallization may oppose structural destabilization and could preserve the integrity of even very thin films. In the case of an A−B diblock where one component crystallizes, there is evidence that, depending on the χN, the diblock copolymer domain structure may be destroyed by crystallization.[17−28]

It is evident from the foregoing discussion that the structure of the molecule largely determines the nature of the intermoleular forces that are active and that these interactions determine the morphology of the film.

* Author to whom correspondence should be addressed. E-mail: green@che.utexas.edu.
[†] Graduate Program in Materials Science and Engineering, The University of Texas at Austin.
[‡] Department of Chemical Engineering, The University of Texas at Austin.
[§] Princeton University.

10.1021/ma0502607 CCC: $30.25
Published on Web 08/13/2005

Table 1. Characteristics of the Crystalline-Amorphous Diblock Copolymer E-*b*-SEB

	bulk	this study
molecular weight, M_n	35.1(kg/mol)	
volume fraction of E block, f_E [a]	0.16	
weight fraction of E block, w_E	0.14	
glass transition temperature of SEB block, T_g °C	25	
crystallization temperature of E block, T_{cr} °C	57	76 ± 1
melting temperature of E block, T_m °C	103	
order−disorder transition temperature, T_{ODT} °C	200	
interaction parameter, χ	$-0.052 + 52.9/T$ (K)	
distance between microdomains, L (nm)	20	21.7 ± 2.2
thickness of the brush layer, Lo (nm)		11.6 ± 1.8

[a] Calculated using method from D. W. Van Krevelen's *Properties of Polymers* (ref 31), $\rho_{PE} = 0.855$ g/cm^3, $\rho_{PS} = 1.05$ g/cm^3, $\rho_{PB} = 0.86$ g/cm^3.

Because the morphology is intimately connected to material performance, an understanding of these issues is critical for the design and processing of thin film polymeric materials for various applications. To this end, it is important to learn how the relative strengths of different forces, ordering, crystallization, and van der Waals forces, determine the structure of a thin film. We examine this question by considering an A_c-*b*-B diblock copolymer in which one component, A_c, is crystallizable. Such a system is particularly attractive because the microstructural details of the system can be controlled through the temperature. This system exhibits an ODT, a melting temperature, and a glass transition temperature. We show that changing the temperature and film thickness determines the relative influence of these three types of molecular interactions on the structure of the film.

Experimental Section

The polyethylene-*b*-poly(styrene-*r*-ethylene-*r*-butene) diblock copolymer (E-*b*-SEB) contains a short polyethylene (E) block connected to a longer styrene-ethylene-butene (70:14:16 by weight) random terpolymer (SEB). The molecular weight of E and SEB blocks are 5 and 30 kg/mol, respectively. The bulk ODT of the copolymer is $T_{ODT} = 200$ °C, the T_g of the amorphous SEB component is $T_g = 25$ °C, and the melting point of the E block is $T_m = 103$ °C. The diblock was synthesized by sequential anionic polymerization of butadiene, then of a styrene/butadiene mixture, followed by catalytic hydrogenation. The E block contains 8 wt % butene because of the microstructure of the precursor polybutadiene.[27] The properties of this copolymer are summarized in Table 1.

Thin films were prepared by dissolving E-*b*-SEB in toluene and spin casting the solutions onto silicon wafers. By controlling spin rate and the concentration of polymer solution, we obtained different thicknesses (ranging from 7 to 200 nm), measured by spectroscopic ellipsometry. Analyses of the topographies of the films were performed in contact mode using an Autoprobe CP scanning force microscope (SFM) from Park Instruments. In some cases, tapping-mode scanning force microscopy measurements were performed using a Nanoscope IV Dimension 3100 (Digital Instruments). Scanning force and optical microscopy images of the films, quenched to room temperature after undergoing heat treatments for specified durations at elevated temperatures under vacuum conditions, revealed the development of a range of topographies that reflect the influence of various interfacial forces. The surfaces of all spin cast films in the above thickness range were smooth prior to annealing.

Results and Discussion

This section is divided into two parts. In the first, topographies of thin films of varying thicknesses, 7 nm $< h <$ 178 nm, annealed at a temperature of 170 °C, were examined. This temperature is above the melting temperatures and below the order−disorder transition

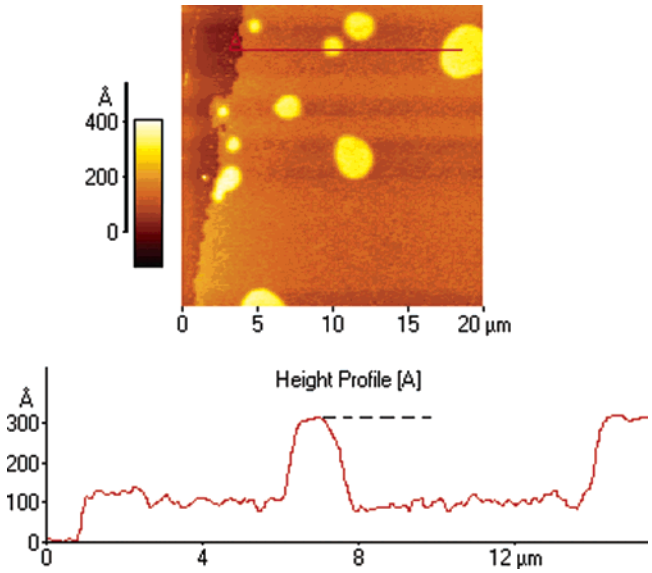

Figure 1. Topographical structure formed by annealing an E/SEB film with $h = 14$ nm at 170 °C for 24 h. The leftmost point shows the position of a scratch and is used as a reference point to measure the height of each layer.

temperatures of the films. This temperature enabled an assessment of the relative influence of the structural forces associated with block connectivity (ordering of the copolymer) versus the long-range van der Waals forces toward the structure of the film; the crystallization forces are active at appreciably lower temperatures. In the second, the effect of crystallization on the structure of films in the thickness range 7 nm $< h <$ 100 nm is examined. While there is evidence of a small film thickness dependence of the crystallization rate and melting temperature, all samples were annealed at $T = 76 \pm 1$ °C as this temperature proved optimal for the development of crystallization within the films (development of crystallization below 70 °C was unreasonably slow in thin films, whereas it is known to be relatively fast in the bulk at this temperature). Our choice of this temperature enabled examination of the relative influence of the three forces, the long-range van der Waals forces, block connectivity, and crystallization, on the structure of the films.

I. Films in the Temperature Range $T_m < T < T_{ODT}$. In this temperature range, the long-range destabilizing van der Waals forces determine the structure of films of thickness $h <$ 12 nm, whereas the structural forces associated with block connectivity determine the structure of films with thickness $h >$ 12 nm. This critical value of h is the thickness of the brush layer $L_0 \cong 12$ nm, and it is also approximately one-half of the bulk

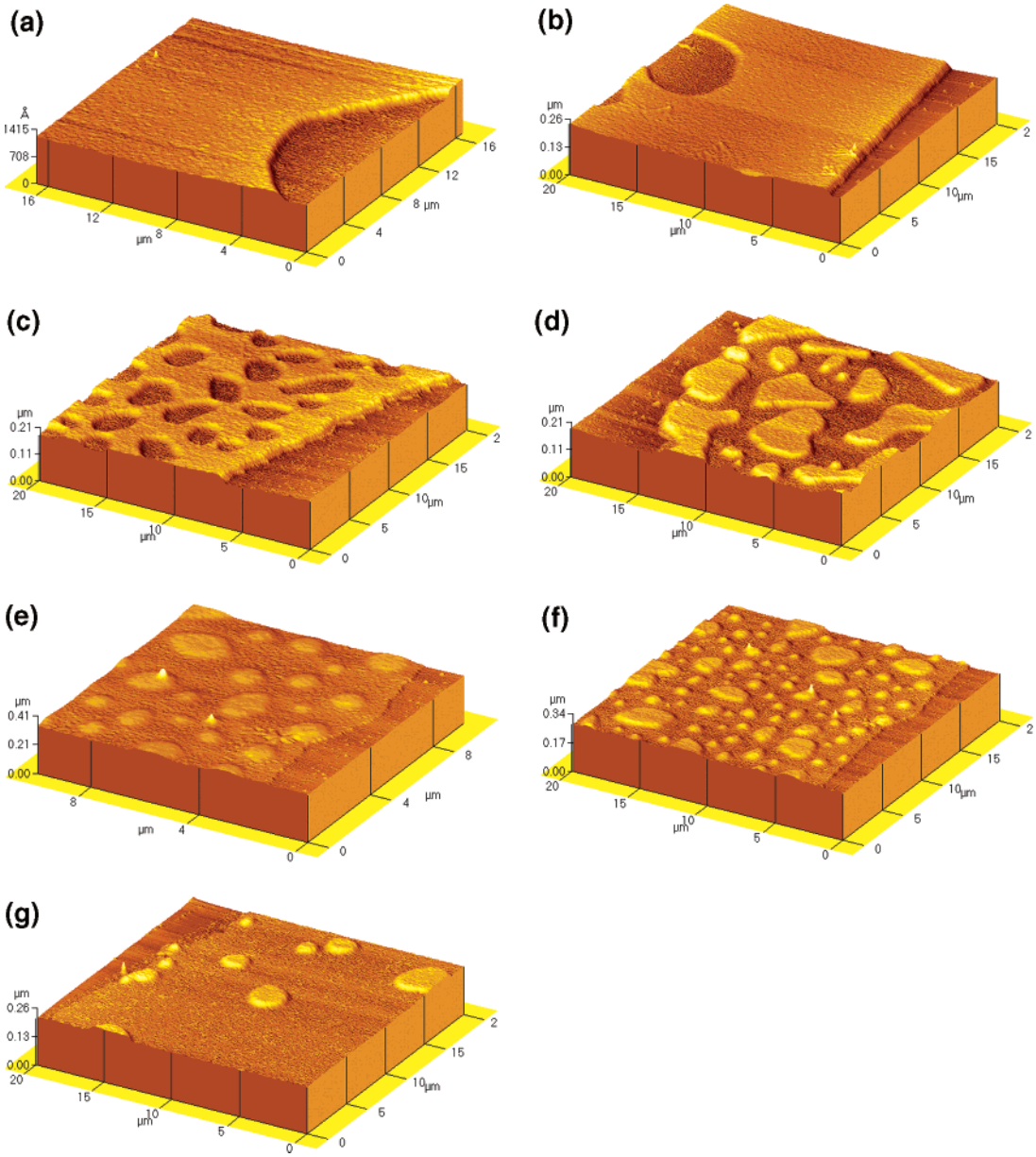

Figure 2. Topographies of samples of varying thickness, annealed at 170 °C. (a) $h = 30$ nm, (b) $h = 28$ nm, (c) $h = 25$ nm, (d) $h = 22$ nm, (e) $h = 19$ nm, (f) $h = 17$ nm, (g) $h = 14$ nm. The edge of each sample contains a scratch made to bare the substrate.

intersphere spacing, $L_0 = L/2$. Section I.a. discusses the structure of films with $h > L_0$, while section I.b. addresses the behavior of films with $h < L_0$.

I.a. Films with Thickness $h > 12$ nm ($h > L_0$). A typical image of the topography of a film annealed at $T = 170$ °C is shown in Figure 1. This sample, whose initial thickness was $h = 14$ nm, was scratched prior to annealing to expose the underlying substrate. Numerous line scans of the sample topography, and of the region containing the scratch, consistently showed that the islands were of height $L = 21.7 \pm 2.2$ nm and that the layer in contact with the substrate was $L_0 = 11.6 \pm 1.8$ nm. A series of images of films ranging in thickness from 30 to 14 nm are shown in Figure 2. The topographies are similar to those formed by symmetric diblock copolymers, and it is well-known that they develop to accommodate the excess material, δh, needed to create a complete layer.[29] The topographies were observed in films ranging in thickness from 30 to 178 nm ($h \sim 8L$). In fact, the SFM tapping mode scans of the edge of the thickest film ($h = 178$ nm) is shown in Figure 3; this film was annealed at 180 °C for 25 h, and the image reveals steps, evidence of order throughout the film.[30]

The bulk phase structure of this diblock is body-centered cubic, where the spheres of E blocks are embedded in a matrix of SEB component.[27,28] In thin films, an asymmetric wetting condition occurs wherein the E component resides at the free surface and the amorphous SEB component resides at the substrate. The surface energies of polyethylene, polystyrene, and polybutene are 36.7, 43.0, and 33.1 mJ/m^2 respectively.[31,32] On the basis of group contribution calculations, the surface energy of the SEB block is 39.4 mJ/m^2, while that of the E block is 36.4 mJ/m^2. Clearly, the E component possesses a lower surface energy than that of the random block, which would indicate that this component should reside at the free surface. The interfacial tension between aromatic hydrocarbons (PS) and polar native oxide is much less than that between completely saturated alkane (PE) chains, so the SEB block resides at the substrate.[33]

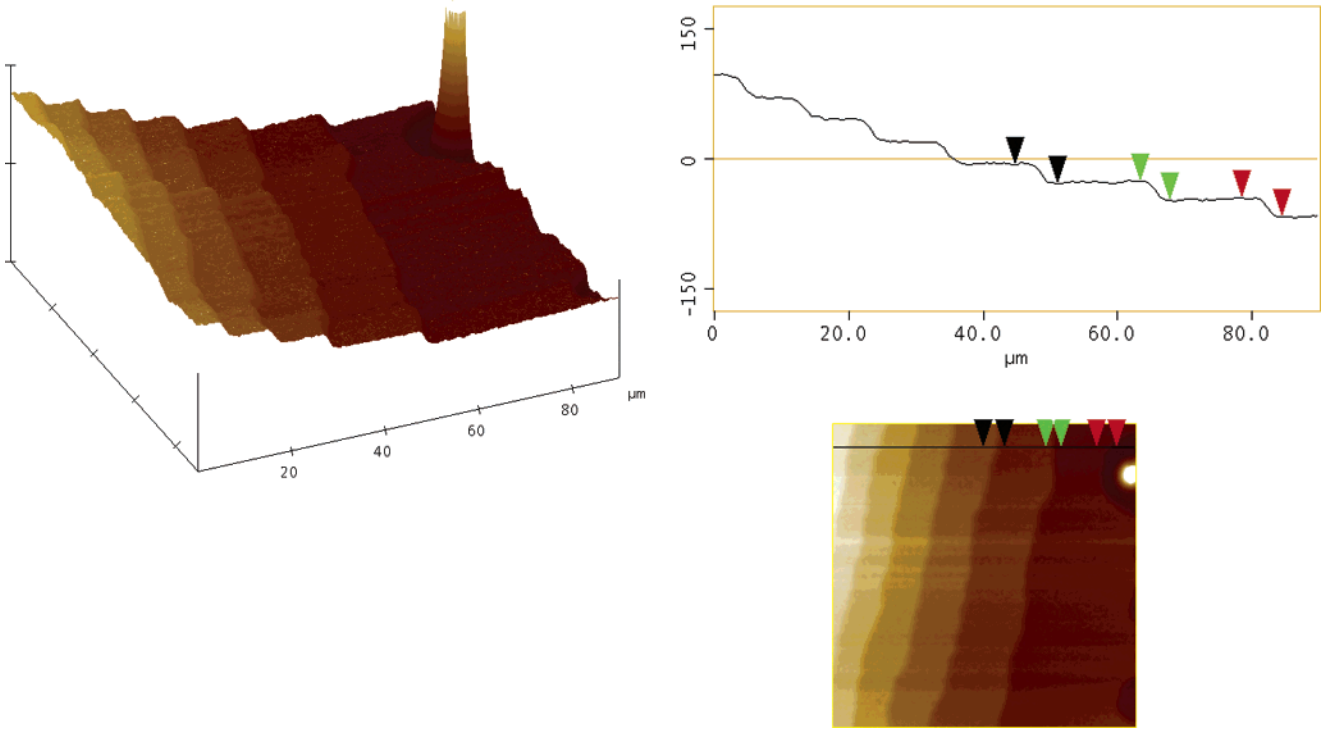

Figure 3. Topographical structure formed by annealing an E/SEB sample of $h = 178$ nm thick at 180 °C for 25 h. The black line in the planar image shows the location of the line scan. Each layer is ~21 nm in height.

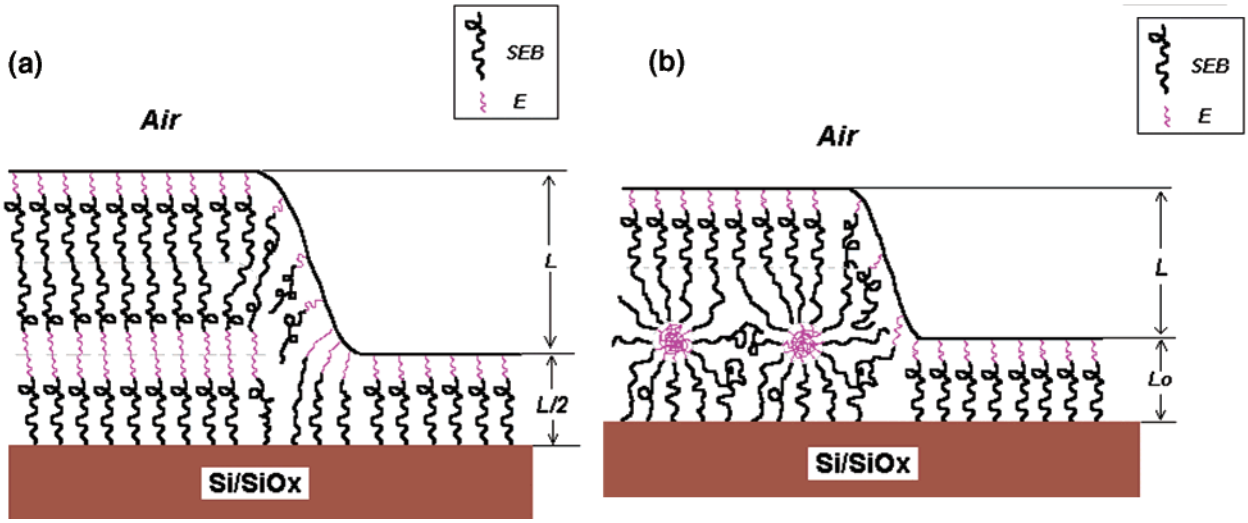

Figure 4. (a) Schematic of the case where a lamellar structure is formed at both surfaces. (b) Schematic of the case where a spherical layer is formed next to the substrate.

Interactions between the substrate and the copolymer segments have been known to modify the structure of the copolymer from hexagonal or spherical to lamellar. Turner et al. examined conditions under which the hexagonal phase of a bulk asymmetric diblock copolymer would be suppressed in favor of a lamellar phase in thin films.[34] For the lamellar region to exist, the free energy penalty associated with the formation of the lamellar phase at the expense of the equilibrium phase, as well as the distortion energy associated with the transition from a lamellar to the equilibrium phase, must be compensated elsewhere. Within a factor of order unity, this occurs when the difference between the surface energies of polymers A and B, $\Delta\gamma$ *is*

$$\Delta\gamma > \gamma_{AB} \tag{1}$$

where γ_{AB} is the interfacial energy between the two blocks, and $\Delta\gamma$ is the difference between the surface energies of the two components of the copolymer. Such a reconstruction from cylinders to lamellae has been observed in the PS-*b*-PDMS system.[35] It turns out that, in this PS-*b*-PDMS system, the criterion specified by eq 1 does indeed predict such a substrate-induced transition, $\Delta\gamma > \gamma_{AB}$ ($\Delta\gamma \cong 23$ mJ/m^2). For the E-*b*-SEB system, $\Delta\gamma = \gamma_A - \gamma_B \cong 3$ mJ/m^2 and an estimate of the interfacial energy is $\gamma_{AB} \sim 1.7$ mJ/m^2,[36,37] which suggests the possibility of a surface-induced lamellar structure. If an E-*b*-SEB film of $h = L_0$ is layered, then how far would the lamellar structure persist in thicker films? If the lamellar structure extends beyond the brush layer, then the structure in Figure 4a arises. However, Figure 4b suggests an alternate possibility that should be considered because eq 1 represents a rough approximation.

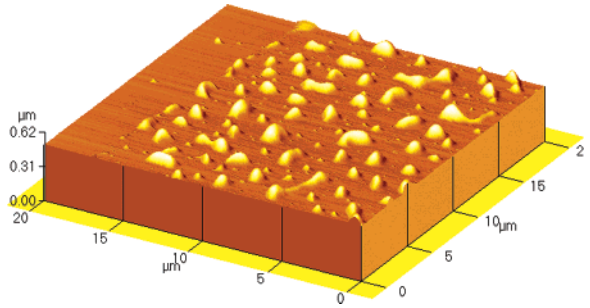

Figure 5. Topographical structure of a sample with $h = 8$ nm ($<L_0$), annealed at 170 °C.

To address this question, it is worthwhile to consider the behavior of an asymmetric polystyrene-*b*-butadiene (PS-*b*-PBD), 65 k:10 k, a diblock copolymer whose interfacial characteristics and asymmetry are similar to those of the E-*b*-SEB copolymer. For example, the minority PBD block wets the free surface of PS-*b*-PBD thin films. On the basis of eq 1, the criterion $\Delta\gamma > \gamma_{AB}$ ($\Delta\gamma = 7.6$ mJ/m^2, $\gamma_{AB} = 0.84$ mJ/m^2, $\gamma_{PS} = 43$ mJ/m^2, and $\gamma_{PBD} = 35.4$ mJ/m^2) would predict a spherical-to-lamellar transition for PS-*b*-PBD thin films. However, unlike the PS-*b*-PDMS copolymer, this transition does not occur, as revealed by an assessment of the experiments of Harrison et al.[33] Spheres are observed beyond the first layer. Therefore, on the basis of the relative surface energies of the E-*b*-SEB copolymer compared to those of the other two copolymers, we expect that Figure 4b best describes the structure of the E-*b*-SEB thin film. The critical issue for this current study is that the samples are ordered in the vicinity of the substrate for films thicker than $L_0 \cong 12$ nm. This is of particular importance in light of the findings of the next section regarding the structure of thinner films at this temperature.

I.b. Films with Thickness below 12 nm ($h < L_0$). The morphology of films with thicknesses $h < L_0$ at $T = 170$ °C ($T_m < T < T_{ODT}$) is now discussed. The E-*b*-SEB films in this thickness range dewet the substrate, forming droplets, as illustrated in Figure 5 for a film of thickness 8 nm. In fact, films of thicknesses 8, 10, and 12 nm dewet the substrate to form droplets. As mentioned earlier, thin liquid films may exist in a morphologically stable, metastable, or unstable state, and this behavior is determined by an effective interface potential.[1–5] For an apolar homopolymer film, this potential is determined by short-range interactions and, more importantly, by long-range van der Waals forces. For this sample, the dewetting is due to destabilizing van der Waals interactions, which may be understood as follows. If a net attraction exists between the interfaces (liquid/vapor and liquid/substrate), then the sample is unstable to local fluctuations of the film thickness. The stability is determined by the curvature of the effective interface potential, where the effective interface potential is

$$\Phi(h) = -\frac{A_{\text{air-poly-SiO}_x}}{12\pi h^2} + \frac{(A_{\text{air-poly-SiO}_x} - A_{\text{air-poly-Si}})}{12\pi(h+d)^2} \quad (2)$$

where $A_{\text{air-poly-SiO}_x}$ and $A_{\text{air-poly-Si}}$ are Hamaker constants, h is the film thickness, and $d \sim 15A$ is the thickness of the SiO_x layer on the surface of the Si wafer. Using Lifshitz theory, we estimate that $A_{\text{air-poly-SiO}_x} = 1.89 \times 10^{-20}$ J and $A_{\text{air-poly-Si}} = -4.92 \times 10^{-20}$ J.[38] On the basis of these values, the curvature of the effective interface potential is negative ($\partial^2\Phi/\partial h^2 < 0$), indicating that there is an attraction between the external interfaces that would lead to destabilization (dewetting) of the film, provided it is sufficiently thin. Because both components are nonwetting on the substrate (negative spreading coefficient, $S < 0$) and the effective Hamaker constant is positive, the final state of the original film would be droplets, as observed.

The oscillatory profile associated with the effective interface potential for the copolymer was not considered explicitly for this calculation. However, it suffices to mention that the first minimum of the potential, corresponding to a stable film thickness, would be at the brush height, 12 nm. The stability of the film would in principle be due to the competition between the destabilizing van der Waals forces and the stability associated with block connectivity that favors a stable film of thickness L_0. If the ordering associated with block connectivity dominated, then the film would have to thicken, and this would happen only if holes developed in the film, as observed in the polystyrene-*b*-poly(methyl methacrylate) (PS-*b*-PMMA) system. The PS-*b*-PMMA copolymer films in the thickness range $h < 12$ nm are relatively more stable because the effective interface potential for this system is different. Specifically, $S > 0$ and the minimum in the potential corresponding to the stable film thickness is 7 nm for the copolymer examined in that study.

In summary, in the temperature range $T_m < T < T_{ODT}$, the morphology of films of $h \geq L_0$ is determined by structural forces associated with chain connectivity, leading to long-range order. For films of h thinner than L_0, the dominance of the destabilizing influence of the van der Waals forces is evident. The minimum of the interface potential of the copolymer denoting a stable film thickness is $L_0 = 12$ nm, and coupled with the fact that in this system $S < 0$, the film forms droplets on the Si/SiO_x substrate. A quantitative assessment of the relative interactions would have to await computer simulations of the entire potential for this system.

II. Effect of Crystallization on the Structure. To understand the effect of forces associated with crystallization, two types of experiments were performed. In the first, films in the thickness range 7 nm $< h <$ 100 nm were isothermally annealed at 76 ± 1 °C; this temperature is above the glass transition of the amorphous component of the copolymer but below the melting temperature of the E block. The samples were subsequently quenched to room temperature and analyzed using SFM. Crystallization is evident in all these films. A second series of films was first isothermally annealed at 170 °C to allow sufficient time for ordering and subsequently quenched to 76 ± 1 °C. At this temperature, crystallization was shown to destroy the topographies associated with copolymer ordering in thicker films. These findings are discussed in parts II.a. and II.b. below.

II.a. Morphology of Samples Annealed in the Temperature Range $T_g < T < T_m$. The samples discussed in this section were annealed at 76 ± 1 °C and allowed to undergo crystallization for various time intervals. Figure 6 shows SFM images of two films, one of thickness $h = 8.5$ nm and the other $h = 11$ nm, that were annealed at 76 ± 1 °C for 5 h. Both films remain

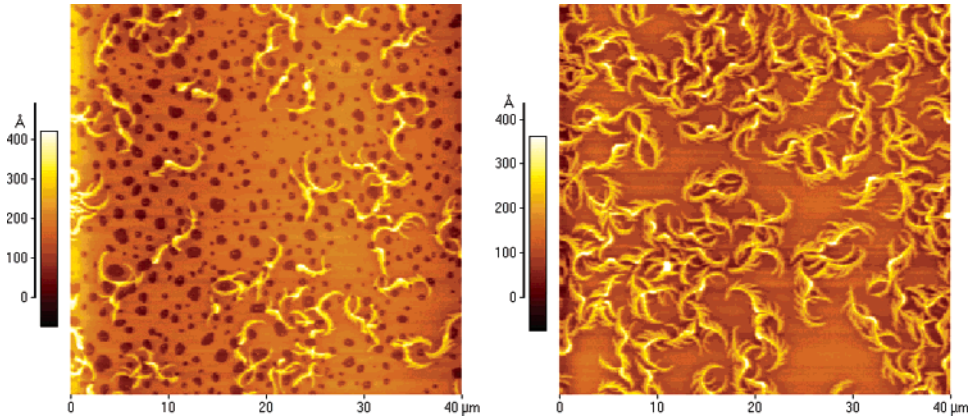

Figure 6. SFM images: (a) a $h = 8.5$ nm E/SEB film crystallized at 77 °C for 5 h, (b) a $h = 11$ nm E/SEB film crystallized at 77 °C for 5 h.

structurally stable with no dewetting. Holes developed throughout the $h = 8.5$ nm sample and appear to be the result of an attempt by the system to decrease its free energy by adjusting its thickness (locally) to L_0, the stable film thickness. This behavior contrasts with that at 170 °C, where droplets developed on the substrate. The thicker $h \approx 11$ nm film, on the other hand, did not contain holes because its thickness is approximately $h \approx L_0$. The topographies of both films are indicative of crystallization. The stabilizing effect on the structure of the film due to crystallization is evident. Morphological stability should not be particularly surprising because energies associated with crystallization are much larger than those attributable to interfacial energies, van der Waals forces, or attributable to phase separation. The energy associated with crystallization ~100 J/g[17,39] and for phase separation it is ~ 1 J/g.[17,40] An estimate of the crystallization energy per unit volume for a polymer with density 1 g/cm^3 is $\sim 10^8$ J/m^3. Considering that the Hamaker constant is $\sim 10^{-20}$ J and the energy per unit area of interaction for a film of thickness 10 nm is $\sim 10^{-5}$ J/m^2, then it should be clear that the film would be stable at this thickness at this temperature largely because of the stabilizing effects of crystallization. We are unable to predict the structure of the film because the relative kinetics of these forces are not well-known. Nevertheless, the topography of the film reveals evidence of some degree of crystallization; the holes in the film suggest evidence of the attempt of the system to form a complete brush layer at the substrate. The stability of the film at this temperature and the absence of stability above T_m are clear indications of the influence of crystallization.

The influence of crystallization on the final morphology of the film increases with increasing film thickness. Three images of the same general region of a film with $h = 33$ nm that was annealed for 23 h at 77 °C are shown in Figure 7. The optical micrograph (Figure 7a) and the SFM image (Figure 7b) indicate that locally one region of the surface is flat, whereas the other region consists of a spherulite structure within a hole. Figure 7c reveals further details about the structure of the film near a region where a scratch exposes the substrate. These measurements show that a brush layer appears close to the edge and its height is h_1. The flat layer on top is of thickness h_2, and the maximum height of the spherulite structure is h_3. We took more than 20 images of samples with an average thickness of 27−40 nm, and for each image, 3 or 4 line scans were chosen. The average values of h_1, h_2, and h_3 obtained from these measurements were compared with L and L_0. It is clear that h_1 (11.2 nm) ~ L and h_2 (33.7 nm) ~ $L_0 + L$. The height h_3 (61.0 nm) bears no relation to any intrinsic morphological features. These results indicate that the microdomain structure is retained near the substrate, whereas the topography reflects evidence of crystallinity at the free surface.

Optical microscope and SFM images of films of thicker films, with $h = 94$ nm and $h = 67$ nm, annealed for 3 h at 75 °C, are shown in Figure 8. The topography of 94 nm film reflects complete crystallization, whereas the topography of the 67 nm film shows evidence of flat regions, indicating incomplete crystallization. The influence of the substrate on crystallization of the film is consistent with observations reported by others. For example, Frank et al. showed that, because of the polymer−substrate interfacial interactions, crystallization of polymers is substantially hindered in thin PEO films with thicknesses below a critical thickness of 15 nm.[41,42]

II.b. Morphology of Films Annealed in Temperature Regime $T_m < T_1 < T_{ODT}$ and Subsequently in the Range $T_g < T_2 < T_m$. Further insight into the relative contributions of crystallization and microdomain formation to the structure of the film may be obtained by first allowing a sample to form an ordered structure at temperatures above T_m and quenching below T_m, where it would crystallize. Figure 9a shows an image of a film of thickness $h = 41$ nm annealed at 170 °C for a sufficiently long time (24 h) to develop a stable phase-separated morphology. The image in Figure 9b is of a sample of identical thickness. However, this sample underwent an additional heat treatment; it was quenched to $T = 76$ °C, where it was allowed to crystallize. It is evident from the images that nucleation at the surface occurs preferentially at the edges of the islands and alters the topography appreciably. This is not surprising because, as mentioned earlier, the crystallization energy is usually larger than the energy associated with microphase separation.

Concluding Remarks

The influence of interfacial constraints and temperature on the self-organization of an asymmetric E-*b*-SEB diblock copolymer, for which the E component is crystallizable, was examined. In the bulk, the equilibrium morphology of this copolymer exhibits bcc symmetry, with E spheres embedded in the SEB matrix.

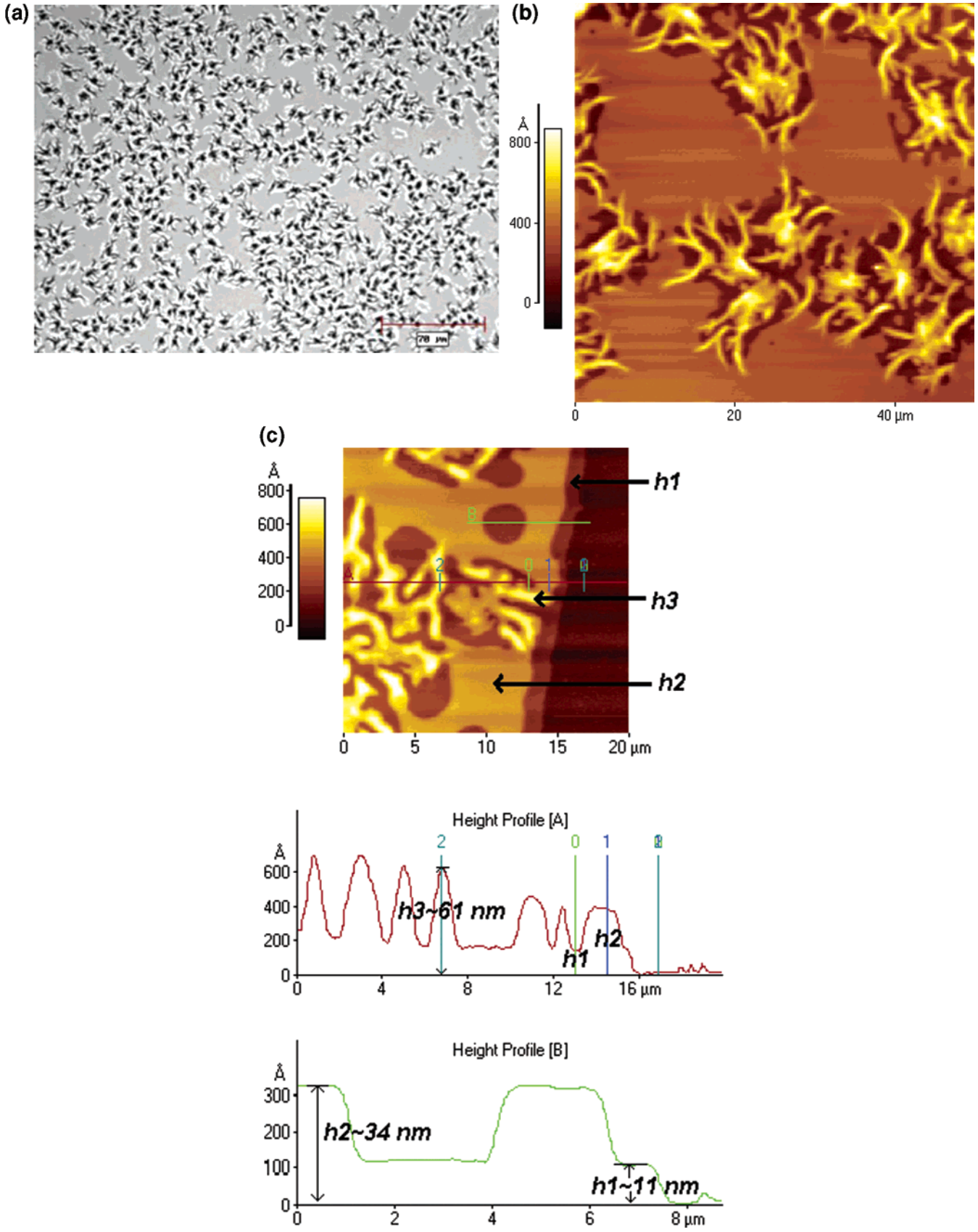

Figure 7. Optical microscopy (a), scanning force topographies (b), and line scans (c) of a film of thickness $h = 33$ nm annealed (crystallized) at 77 °C for 23 h. The parameters identified in the diagram are $h_1 = 11.2 \pm 1.5$ nm ($\sim L_0$), $h_2 = 33.7 \pm 2.4$ nm ($\sim L+L_0$), and $h_3 = 61.0 \pm 3.0$ nm.

Throughout the temperature range $T_m < T < T_{ODT}$, in thin films ($h > 12$ nm) supported by SiO_x/Si substrates, an ordered, terraced structure is observed, indicating the dominance of the driving forces for ordering as in a typical block copolymer. Films thinner than 12 nm were structurally unstable; they dewet, and formed droplets

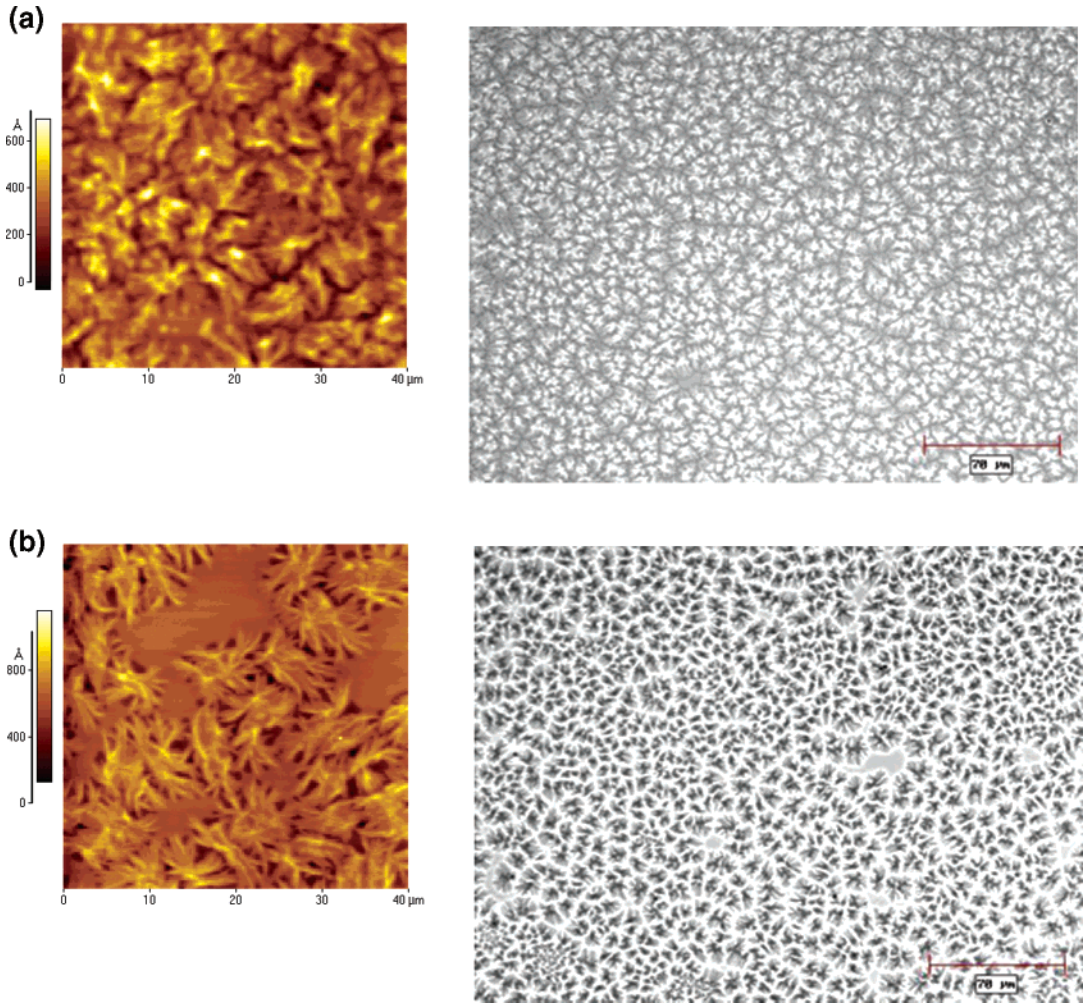

Figure 8. Optical microscopy (right) and SFM images (left) of samples crystallized at 76−77 °C: (a) $h = 94$ nm film crystallized at 75 °C for 3 h, (b) $h = 67$ nm film crystallized at 75 °C for 3 h.

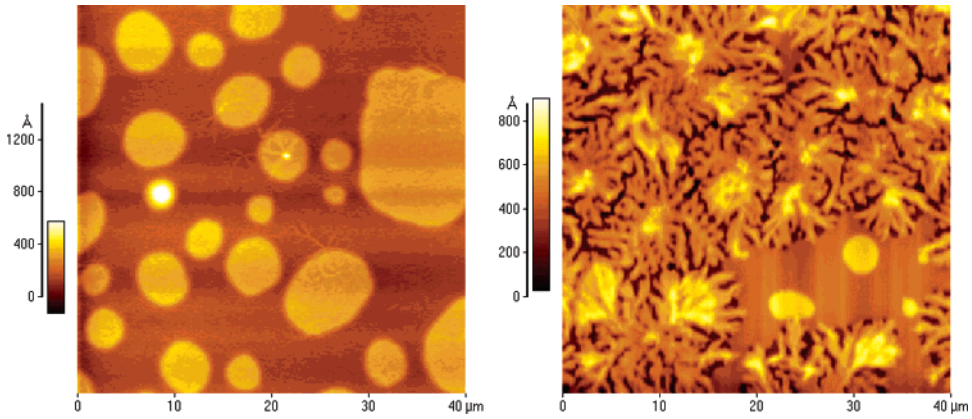

Figure 9. SFM images: (a) a $h = 41$ nm E/SEB film annealed at 170 °C for 24 h, (b) a $h = 41$ nm E/SEB film annealed at 170 °C for 3 h and then crystallized at 75 °C for 3 h.

on the substrate. This instability was due to long-range van der Waals forces. All films annealed within the temperature range $T_g < T < T_m$, remained structurally stable, and the stability is largely associated with crystallization (films of $h < 12$ nm were also stable). Crystallization destroyed the microdomain morphology; this was particularly evident in thicker films, where the influence of the substrate is smaller than that for thinner films. Specifically, the layered structure, steps, was evident in films of thickness below or about 33 nm. In thicker films, they were completely eradicated by crystallization. A more quantitative assessment of the relative influence of interfacial forces on the structure of thin films awaits simulations.

Acknowledgment. This work was supported by the National Science Foundation, Polymers Program (DMR-0072897 to P.F.G. and DMR-0220236 to R.A.R.), NSF-STC-CHE-9876674, and the Robert A. Welch Foundation.

References and Notes

(1) Green, P. F. *J. Polym. Sci., Part B: Polym. Phys.* **2003**, *41,* 2219.
(2) Brochard-Wyart, F.; Debregeas, G.; Fondecave, R.; Martin, P. *Macromolecules* **1997**, *30*, 1211.
(3) Reiter, G. *Langmuir* **1993**, *9*, 1344.
(4) Seemann, R.; Herminghaus, S.; Jacobs, K. *Phys. Rev. Lett.*, **2001**, *86*, 5534.
(5) Sharma, A.; Reiter, G. *J. Colloid Interface Sci.* **1996**, *178*, 383.
(6) Hamley, I. W. *The Physics of Block Copolymers*; Oxford University Press: New York, 1998.
(7) Bates, F. S.; Fredrickson, G. H. *Annu. Rev. Phys. Chem.* **1990**, *41*, 525.
(8) Hamley, I. W. *Adv. Polym. Sci.* **1999,** *148,* 113.
(9) Fasolka, M. J.; Mayes, A. M. *Annu. Rev. Mater. Res*. **2001**, *31*, 323.
(10) De Rosa, C.; Park C.; Thomas, E. L.; Lotz B. *Nature* **2000**, *405*, 433.
(11) Volkmuth, W. D.; Austin, R. H. *Nature* **1992**, *358*, 600.
(12) Chou, S. Y.; Wei, M. S.; Krauss, P. R.; Fischer, P. B. *J. Appl. Phys*. **1994**, *76*, 6673.
(13) Fink, Y.; Winn, J. N.; Fan, S.; Chen, C.; Michel, J.; Joannopoulos, J. D.; Thomas, E. L. *Science,* **1998,** *282*, 1679.
(14) Park, M.; Harrison, C.; Chaikin, P. M.; Register, R. A.; Adamson, D. H. *Science*, **1997**, *276*, 1401.
(15) Flory, P. G. *Scaling Concepts in Polymer Physics*; Cornell University Press: Ithaca, New York, 1979.
(16) Shull, K. R. *Macromolecules* **1996**, *29*, 8487.
(17) Loo, Y. L. Templating Polymer Crystal Growth on a Nanoscale Using Phase-Separated Block Copolymers. In *The Encyclopedia of Nanoscience and Nanotechnology;* Marcel Dekker: New York, 2002.
(18) Reiter, G. *J. Polym Sci., Part B: Polym. Phys.* **2003**, *41*, 1869.
(19) Reiter, G.; Castelein, G.; Sommer J. U. *Phys. Rev. Lett.*, **2001**, *87*, 226101.
(20) Reiter, G.; Castelein, G.; Hoerner, P.; Riess. G.; Bluman, A.; Sommer J. U. *Phys. Rev. Lett.* **1999**, *83*, 3844.
(21) Reiter, G.; Castelein, G.; Hoerner, P.; Riess. G.; Sommer, J. U.; Floudas, G. *Eur. Phys. J. E* **2000**, *2*, 319.
(22) Opitz, R.; Lambreva, D. M.: de Jeu, W. H. *Macromolecules* **2002**, *35*, 6930.
(23) Hong, S.; Macknight, W. J.; Russell, T. P.; Gido, S. P. *Macromolecules* **2001**, *34*, 2876.
(24) Hamley, I. W.; Wallwork, M. L.; Smith D. A.; Fairclough L. P. A.; Ryan A. J.; Mai S. M.; Yang Y. W.; Booth C. *Polymer* **1998**, *39*, 3321.
(25) Zhang, F.; Chen, Y.; Huang, H.; Hu, Z.; He, T. *Langmuir* **2003**, *19*, 5563.
(26) Zhang, F.; Huang, H.; Hu, Z.; Chen, Y.; He, T. *Langmuir* **2003**, *19*, 10100.
(27) Loo, Y. L.; Register, R. A.; Ryan, A. J. *Phys. Rev. Lett.* **2000**, *84*, 4120.
(28) Loo, Y. L.; Register, R. A.; Ryan, A. J. *Macromolecules* **2002**, *35*, 2365.
(29) Russell, T. P. *Curr. Opin. Colloid Interface Sci.* **1996**, *1,* 107.
(30) Orso, K. A.; Green, P. F. *Macromolecules*, **1999**, *32*, 1087.
(31) Van Krevelen, D. W. *Properties of Polymers*; Elsevier Science: New York, **1976.**
(32) On the basis of ref 31, we estimate the surface tension using an additive function, $\gamma = (Ps/V)^4$, in which Ps is molar parachor and V is molar volume. The values of Ps and V are calculated using group contribution. For example, for polybutylene $Ps(\mathrm{PB}) = 39(\mathrm{CH_2}) \times 2 + 56.1(\mathrm{CH_3}) + 17.1(\mathrm{C}) + 4.8(\mathrm{H}) = 156.0$, $V(\mathrm{PB}) = 9.45(\mathrm{CH}) + 15.85(\mathrm{CH_2}) \times 2 + 23.9(\mathrm{CH_3}) = 65.05$, so $\gamma = (156/65.05)^4 = 33.1$. All these calculated values agree with Table 5 in comprehensive tables part of ref 31.
(33) Harrison, C.; Park, M.; Chaikin, P. M.; Register, R. A.; Adamson, D. H.; Yao, N.; *Polymer*, **1998**, *39*, 2733.
(34) Turner, M. S.; Rubinstein, M.; Marques, C. M. *Macromolecules* **1994**, *27*, 4986.
(35) Chen X.; Gardella, J. A. Jr.; Kumler P. A. *Macromolecules* **1992**, *25*, 6631.
(36) Wu, S. *Polymer Interface and Adhesion*; Marcel Dekker: New York, 1982.
(37) From eq *8.12* in ref 31, $\gamma_{AB} \approx \gamma_A + \gamma_B - 2\phi_{AB}(\gamma_A\gamma_B)^{1/2}$, and $\Phi_{AB} = 4(V_AV_B)^{1/3}/(V_A^{1/3} + V_B^{1/3})^2$, $V(\mathrm{SEB}) = 83.45$, and $V(\mathrm{E}) = 34.37$, so $\Phi_{AB} = 0.978$ and $\gamma_{AB} = 1.7$ mJ/m^2. Table 3.14 of ref 36, gives the value of interfacial energies between polystyrene and polyethylene is 5.1 mJ/m^2 at 180 °C, which is significantly larger than the above estimation. This is partly due to the fact that the polyethylene chains in SEB block can contact with E block to minimize the unfavorable chain contact between polystyrene and polyethylene, thus a smaller interfacial energy is expected for E-SEB than polystyrene−polyethylene. In fact, using the same method as above, the γ_{AB} value between polystyrene−polyethylene is 3.1 mJ/m^2, which is much larger than 1.7 mJ/m^2.
(38) $A_{132} = (\sqrt{A_{11}} - \sqrt{A_{33}})(\sqrt{A_{22}} - \sqrt{A_{33}})$, $A_{\mathrm{Si-Si}} = 21.1 \times 10^{-20}$ J, $A_{\mathrm{SiO_x}} - \mathrm{SiO_x} = 5 \times 10^{-20}$ J. The Hamaker constant of polymer can be estimated by $A = 3/4\ kT((\epsilon_1 - 1)/(\epsilon_1 + 1))^2 + (3h\nu_e)/(16\sqrt{2})(n_1^2 - 1)^2)/((n_1^2 - 1)^{3/2})$. Here n is the refractive index, ϵ is the dielectric permittivity of the polymer, and ν_e is the main electric absorption frequency in the UV, typically around 3×10^{15} s^{-1}. From ref 31, $n_{\mathrm{PS}} = 1.591$, $n_{\mathrm{PE}} = 1.49$, $n_{\mathrm{PB}} = 1.5125$, $\epsilon_{\mathrm{PS}} = 2.55$, $\epsilon_{\mathrm{PE}} = 2.3$, $\epsilon_{\mathrm{PB}} = 2.2$. According to Lorentz−Lorenz ideal mixing rule, $(n_{\mathrm{mix}}^2 - 1)/(n_{\mathrm{mix}}^2 + 2) = \sum \Phi_i\,(n_i^2 - 1)/(n_i^2 + 2)$ and $((\epsilon_{\mathrm{mix}}^{1/2} - 1)^2)/((\epsilon_{\mathrm{mix}}^{1/2} + 2)^2) = \sum \Phi_i\,((\epsilon_i^{1/2} - 1)^2)/((\epsilon_i^{1/2} + 2)^2)$. Here, Φ_i is the volume fraction of each component, $n_{\mathrm{E/SEB}} = 1.55$, and $\epsilon_{\mathrm{E/SEB}} = 2.42$, so $A_{\mathrm{poly-poly}} = 8.34 \times 10^{-20}$ J and $A_{\mathrm{air-poly-SiO_x}} = 1.89 \times 10^{-20}$ J and $A_{\mathrm{air-poly-Si}} = -4.92 \times 10^{-20}$ J. More detail information about this calculation can be found in (a) Meli, L.; Pham, J. Q.; Johnston, K. P.; Green, P. F. *Phys. Rev. E* **2004**, *69*, 051601; (b) Abramowitz, H.; Shah, P. S.; Green, P. F.; Johnston, K. P. *Macromolecules* **2004**, *37*, 7316.
(39) *Polymer Handbook*; Brandrup, J., Immergut, E. H., Eds.; Wiley: New York, 1989.
(40) Stuhn B. *J. Polym. Sci., Part B: Polym. Phys.* **1992**, *30*, 1013.
(41) Frank, C. W.; Rao, V.; Despotopoulou, M. M.; Pease, R. F. W.; Hinsberg, W. D.; Miller, R. D.; Rabolt, J. F. *Science* **1996**, *273*, 912.
(42) Despotopoulou, M. M.; Frank, C. W.; Miller, R. D.; Rabolt, J. F. *Macromolecules* **1996**, *29*, 5797.

MA0502607